Controlled Free-Radical Polymerization of *n*-Butyl Acrylate by Reversible Addition−Fragmentation Chain Transfer in the Presence of *tert*-Butyl Dithiobenzoate. A Kinetic Study

Elena Chernikova,[†,‡] Andrey Morozov,[†] Ekaterina Leonova,[†] Elizaveta Garina,[†] Vladimir Golubev,[†] Chuong Bui,[‡] and Bernadette Charleux*[,‡]

Polymer Department, Faculty of Chemistry, Lomonosov Moscow State University, Leninskie Gori, 117899, Moscow, Russia, and Laboratoire de Chimie des Polymères, Unité de recherche associée au CNRS (UMR7610), Université Pierre et Marie Curie, Tour 44, 1er étage, 4, Place Jussieu, 75252 Paris Cedex 05, France

Received February 4, 2004; Revised Manuscript Received June 22, 2004

ABSTRACT: The RAFT polymerization of *n*-butyl acrylate was studied in the presence of various concentrations of *tert*-butyl dithiobenzoate (t-BDB) as a chain transfer agent, and various concentrations of AIBN as an initiator at 60 and 90 °C. The polymerizations exhibited the expected features of controlled systems. In particular, the linear increase in number-average molar mass (M_n) with monomer conversion, from very low conversion values, indicated a large apparent chain transfer constant to t-BDB. The kinetic study showed two typical characteristics already observed in RAFT polymerizations of various acrylates: the existence of an induction period and a strong rate retardation, both enhanced by the increase in t-BDB initial concentration. ESR spectroscopy was applied at 90 °C and revealed the existence of an unexpectedly large concentration of intermediate radicals. The system was examined and discussed considering either the possibility of cross-termination between a propagating macroradical and an intermediate one, with fast fragmentation of the intermediate radicals or the absence of cross-termination but slow fragmentation.

Introduction

A wide variety of well-defined homopolymers and copolymers with complex architectures have become easily accessible since the advent of controlled free-radical polymerization (CRP).[1−3] Several methods are available such as nitroxide-mediated polymerization (NMP),[4] atom transfer radical polymerization (ATRP),[5,6] and reversible transfer techniques (reversible addition−fragmentation chain transfer, RAFT,[7−11] and macromolecular design via the interchange of xanthates, MADIX[12]). The reversible transfer methods based on addition−fragmentation reaction are particularly versatile as they allow to control the homopolymerization of a great variety of monomers[7−15] such as styrenics, acrylates, methacrylates, vinyl esters, and polar or water-soluble monomers such as acrylamides[16−18] and acrylic acid.[7,8,19,20] Control operates via the introduction of a specific chain transfer agent (CTA) into the polymerization medium. In the RAFT and MADIX methods these CTA have in common to contain a thiocarbonylthio function, and their structure can be schemed as Z−C(═S)−S−R with Z the activating group and R the leaving/initiating group. The admitted transfer mechanism follows two steps. The first one is the addition of a propagating radical P• to the C═S double bond of the CTA, which leads to an adduct radical P−S−C•(Z)−S−R. The second step corresponds to fragmentation of this intermediate radical into R• and the Z−C(═S)−S−P dormant species. The latter also plays the role of a CTA, undergoing the same addition−fragmentation reactions as the Z−C(═S)−S−R initial compound via a P−S−C•(Z)−S−P intermediate radical (Scheme 1). For the so-called RAFT method the CTA can be dithioesters (Z = alkyl or aryl), trithiocarbonates (Z = R′S−), and dithiocarbamates (Z = R′R″N−), whereas MADIX requires the use of xanthates (i.e., dithiocarbonates, Z = R′O−). The great diversity of the RAFT agents comes from the possible combination of various Z and R groups. The activity of such molecules in controlling the free-radical polymerization process strongly depends on the nature of R, of Z, and of the selected monomer.[10,11]

Kinetics of the polymerizations based on the RAFT process have been extensively studied, in particular for styrene, and an important aspect, commonly revealed by literature data, is the significant rate retardation.[10,11,13,14] The reason for this retardation is not completely clear so far. On one hand, slow fragmentation of the initial intermediate radical (see Scheme 1) and/or the influence of the nature of the leaving group (such as slow reinitiation) were suggested to be responsible for this phenomenon.[21−24] Actually, the ongoing debate mainly focuses on the magnitude of the fragmentation rate constant.[25,26] On the other hand, the possibility of irreversible or reversible termination (by combination[27] or possible disproportionation[28]) of the intermediate radical with another (macro)radical in the polymerization medium was put forward.[27−33] To this point, a definitive conclusion is still expected since experimental indications supporting either the existence[27,31−33] or the absence[28] of cross-termination products were reported. A study devoted to the early stage of the polymerization of styrene in the presence of cyanoisopropyl dithiobenzoate showed that the first addition step to the RAFT agent was extremelly selective (called initialization period).[34] During that step the RAFT agent was almost completely converted into its single monomer adduct before the formation of larger molar mass living chains. For this reason, in a system where the rate constant of addition of the initiating

[†] Lomonosov Moscow State University.
[‡] Université Pierre et Marie Curie.

10.1021/ma049757r CCC: $27.50
Published on Web 07/30/2004

Scheme 1. Mechanism of Polymerization Based upon Reversible Addition−Fragmentation Chain Transfer

A- Chain transfer of primary radical to t-BDB:

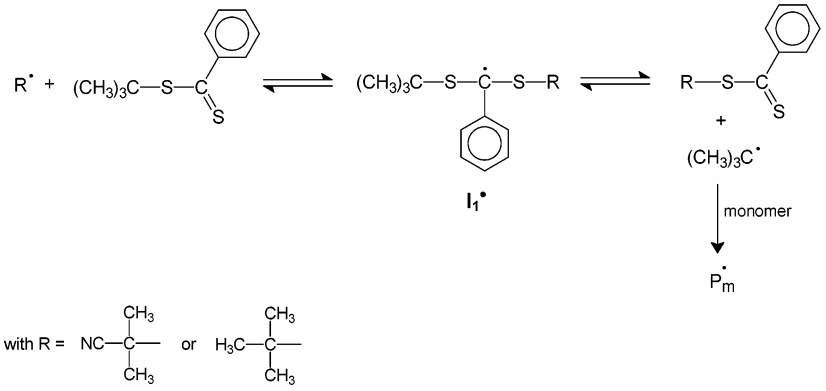

B- Chain transfer of macroradical to t-BDB (pre-equilibrium):

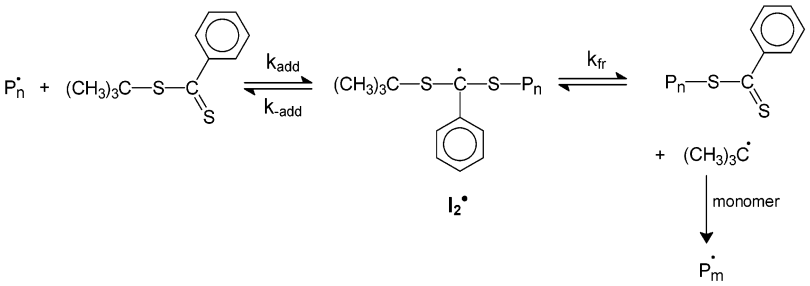

C- Chain transfer of macroradical to poly(n-butyl acrylate) with dithiobenzoate end-group (core equilibrium):

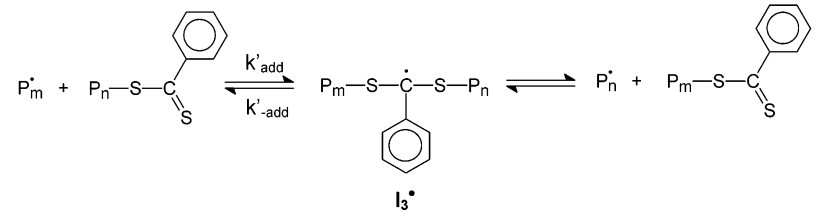

radical (leaving radical from the RAFT agent) to the monomer would be lower than the rate constant of propagation, an induction period might then be observed.

In comparison to styrene, much less work has been devoted to the polymerization kinetics of other monomers. For instance, the features of the polymerization of acrylates, which represent an important class of monomers, have already been reported, but generally as part of a more general study.[7−15,35] Only a very small number of articles exclusively focused on acrylate RAFT polymerization, in particular methyl acrylate[28,36−38] and *n*-butyl acrylate.[39] All of these articles reported very similar characteristics as far as polymerization kinetics were concerned. In general, with most RAFT agents used, polymerizations led to well-controlled homopolymers with predictable molar mass and narrow molar mass distribution due to very large chain transfer constants. In some cases, a bimodal SEC (size exclusion chromatography) distribution has been observed at high conversion,[10,13,14] depending on the nature of the RAFT agent (i.e., with chain transfer agents exhibiting very large chain transfer constants, the final polymer had sufficiently narrow molar mass distribution to reveal the existence of a shoulder on the high molar mass side of the SEC peak).[14] These high molar mass homopolymers were still living as they retained the dithiobenzoate group, which precludes their simple formation by irreversible coupling between propagating macroradicals.[14] Polymerizations were found to be very slow with respect to reactions carried out in the absence of chain transfer agent. Indeed, more than 10 h was typically required to reach high conversions.[14,36,38,39] This was particularly true when dithiobenzoate RAFT agents were used. Indeed, changing to a transfer agent with dithioacetate or phenyldithioacetate functionality enabled the polymerization to be faster and even controlled at ambient temperature.[37] Polymerization rate significantly decreased when the amount of RAFT agent was increased. In addition, a long induction period was observed,[38] the duration of which increased when the concentration of RAFT agent was increased. Induction and retardation were correlated to the structure of the RAFT agent, in particular that of the R leaving group in dithiobenzoate transfer agents, as exemplified by the work of Perrier et al.[38] Indeed, the longer induction periods were observed in this order: R = cumyl (complete inhibition at 60 °C) > phenylethyl > cyanoisopropyl, although the reverse would be expected on the basis of the stability of the leaving radical itself. In contrast,

no induction period was observed with a poly(methyl acrylate) macro-RAFT agent. All of these results allowed the authors to conclude that slow fragmentation of the first intermediate radical was responsible for this induction period.

This work is devoted to the kinetic study of the RAFT homopolymerization of *n*-butyl acrylate in the presence of *tert*-butyl dithiobenzoate as a reversible chain transfer agent. Such transfer agent has not been used very often.[40−43] In particular, it has never been used for the homopolymerization of alkyl acrylates, only in the random copolymerization of methyl acrylate with vinylidene chloride,[42] in which it induced a severe rate retardation when compared with other dithiobenzoate RAFT agents such as benzyl dithiobenzoate and 1-(ethoxycarbonyl)eth-1-yl dithiobenzoate. The purpose of this work is to examine the kinetic features of such polymerization and to understand the reasons for the induction and rate retardation phenomena.

Experimental Part

Materials. *n*-Butyl acrylate (*n*-BuA, Acros, 99%) was distilled under vacuum before use. Azobis(isobutyronitrile) (AIBN, Aldrich, 99%) was recrystallized from ethanol and dried under vacuum. *tert*-Butylmercaptan (Aldrich, 99%) and *S*-(thiobenzoyl)thioglycolic acid (Aldrich, 99% purity) were used as received. Benzene (SDS, 99.5%) and tetrahydrofuran (THF, Prolabo, 99%) were distilled on CaH_2 before use.

Synthesis of *tert*-Butyl Dithiobenzoate (t-BDB). Synthesis of the *tert*-butyl dithiobenzoate RAFT agent was performed according to a procedure previously described in the literature.[19] *S*-(Thiobenzoyl)thioglycolic acid (10.6 g, 0.05 mol) was dissolved in dilute alkaline solution containing 2 equiv of NaOH (4.0 g, 0.1 mol in 400 mL of H_2O). Then, *tert*-butylmercaptan (4.95 g, 0.055 mol) was added under stirring at room temperature. The mixture was stirred for a period of 15 h. Afterward, *tert*-butyl dithiobenzoate, which separated out as a heavy, dark, pink oil, was extracted with ether (1 × 600 mL, 1 × 300 mL). The organic extracts were washed with 0.1 N aqueous NaOH (3 × 300 mL) and water (3 × 300 mL), then dried over $MgSO_4$, filtered, and evaporated. Then the product was left overnight under vacuum (0.01 mmHg, 40 °C) to eliminate the residual *tert*-butylmercaptan (bp = 63 °C). The yield of *tert*-butyl dithiobenzoate (t-BDB), which remained as a dark pink oil after purification, was 90%. ^{1}H NMR (d_6-acetone; 200 MHz) δ (ppm): 1.69, 7.34, 7.47, 7.87. ^{13}C NMR (d_6-acetone; 50 MHz) δ (ppm): 28.24, 52.63, 127.19, 128.91, 132.64, 147.71, 231.10. ^{1}H and ^{13}C NMR did not reveal the presence of extra peaks, which indicates the absence of impurities that could be accurately quantified.

Polymerization Conditions. For investigation of the influence of t-BDB on the polymerization kinetics, the solution containing AIBN (10^{-3} mol L^{-1}) in freshly distilled *n*-BuA was prepared first, and then this solution was added to a selected amount of t-BDB. Changing t-BDB concentration was achieved by diluting the prepared reaction mixture (AIBN, t-BDB, *n*-BuA) with the initial solution of AIBN in monomer. For investigation of the influence of AIBN on kinetics, the reaction mixtures were prepared according to the same procedure, but keeping t-BDB concentration the same (10^{-2} mol L^{-1}) and varying AIBN concentration. Afterward, a known amount of each solution was poured into an ampule (approximately 0.2 mL) and degassed down to 5×10^{-3} mmHg residual pressure using four freeze−vacuum−thaw cycles. The ampules were immersed, for the required period of time, into an oil bath thermostated at 60 or 90 °C. After polymerization, the reaction mixtures were cooled in liquid nitrogen and diluted with benzene. The polymers were extracted by lyophilization from benzene.

Samples for ESR experiments were prepared similarly; the amount of reaction mixture in the ampule was 70 μL.

Table 1. Experimental Conditions for the Various Polymerizations of *n*-Butyl Acrylate in Bulk, Initiated by AIBN in the Presence of *tert*-Butyl Dithiobenzoate

expt	temp (°C)	$[AIBN]_0$ (mol L^{-1})	$[t\text{-}BDB]_0$ (mol L^{-1})
1a	60	1×10^{-3}	1×10^{-1}
1b	60	1×10^{-3}	3×10^{-2}
1c	60	1×10^{-3}	1×10^{-2}
1d	60	1×10^{-3}	3×10^{-3}
1e	60	1×10^{-3}	1×10^{-3}
1f	60	1×10^{-3}	3×10^{-4}
1g	60	1×10^{-3}	0
2a	60	3×10^{-2}	1×10^{-2}
2b	60	1×10^{-2}	1×10^{-2}
2c	60	3×10^{-3}	1×10^{-2}
2d	60	1×10^{-3}	1×10^{-2}
2e	60	3×10^{-4}	1×10^{-2}
3a	90	1×10^{-3}	1×10^{-1}
3b	90	1×10^{-3}	3×10^{-2}
3c	90	1×10^{-3}	1×10^{-2}
3d	90	1×10^{-3}	3×10^{-3}
3e	90	1×10^{-3}	1×10^{-3}
3f	90	1×10^{-3}	3×10^{-4}
3g	90	1×10^{-3}	0
4a	90	3×10^{-2}	1×10^{-2}
4b	90	1×10^{-2}	1×10^{-2}
4c	90	3×10^{-3}	1×10^{-2}
4d	90	1×10^{-3}	1×10^{-2}
4e	90	3×10^{-4}	1×10^{-2}
4f	90	1×10^{-4}	1×10^{-2}
5a	90	1×10^{-1}	3×10^{-1}
5b	90	3×10^{-2}	3×10^{-1}
5c	90	1×10^{-2}	3×10^{-1}
5d	90	3×10^{-3}	3×10^{-1}
6	90	1×10^{-2}	1×10^{-1}
7	90	1×10^{-2}	3×10^{-2}

The experimental conditions are summarized in Table 1.

Polymerization Kinetics. Polymerization kinetics was investigated at the Polymer Department of Moscow State University using a Calvet type differential automatic calorimeter DAK-1-1a. An ampule containing 0.2 mL of the polymerization medium was put into the working cell. Another ampule containing the same volume of a previously polymerized reaction medium was put in the reference cell. The amount of released heat was measured in isothermal conditions at 60 or 90 °C. The conversions were calculated by integration of the calorimetric curves, using the molar enthalpy of *n*-butyl acrylate polymerization:[44] $\Delta H = -76$ kJ mol^{-1}. For all experiments, gravimetry was used to measure conversion of the samples selected for molar mass analysis.

Analytical Techniques. Average molar mass and molar mass distribution of the polymers were measured by size exclusion chromatography (SEC). The analyses were carried out in THF solution. For experiments 1a, 1c, 3a, and 3c they were carried out at 40 °C, with a flow rate of 1 mL min^{-1}. Separation was performed using a GPC Vorsaule PSS SDV 8 × 300 mm, 5 μm, linear column. The apparatus is equipped with a refractive index detector (LDC Analytical refractoMonitor IV), a UV detector operating at 254 nm (Waters 484), a Viscotek VE 7510 GPC degasser, a Waters 515 pump, and a Viscotek VE 5200 autosampler. Chromatograms were recorded using the TriSec Data Acquisition System software from Viscotek. Molar masses were derived from a calibration curve based on polystyrene standards (300−1.09×10^6 g mol^{-1}),[45] and calculation was performed using the TriSec 3.0 GPC Software from Viscotek. For experiments 1b, 1c, 3b, and 3c some analyses (at medium and high conversions) were carried out at 35 °C with a flow rate of 0.9 mL min^{-1}, using a Waters liquid chromatograph equipped with a RI410 refractive index detector and three columns packed with Ultrastyragel with pore dimensions 10^4 and 10^5 Å and a Waters Styragel HR 5E linear column (2000−4×10^6 g mol^{-1}). Chromatograms were processed with a Data Module-730 integrator using calibration curve based on polystyrene standards.

Polymers obtained in experiment 3a were analyzed by MALDI−TOF mass spectrometry performed using a

PerSeptive Biosystems Voyager Elite (Framingham, MA) time-of-flight mass spectrometer. This instrument is equipped with a nitrogen laser (337 nm, 3 ns pulse), a delayed extraction, and a reflector. It was operated at an accelerating potential of 25 kV in reflector mode. The MALDI−TOF mass spectra represent averages over 2048 consecutive laser shots (3 Hz repetition rate). The polymer solutions (2−5 g L^{-1}) were prepared in THF. The matrix, 1,8-dihydroxy-9[10*H*]-anthracenone (dithranol), was also dissolved in THF (25 g L^{-1}). A 10 μL portion of the polymer solution was mixed with 20 μL of the matrix solution. A sodium iodide solution (10 μL of a solution at 20 g L^{-1} in THF) was finally added to favor ionization by cation attachment. A 1 μL portion of the final solution was deposited onto the sample target and allowed to dry in air at room temperature. Polystyrene standards of known structure (purchased from Polymer Standards Service) were used to calibrate the mass scale using the two-point calibration software 3.07.1 from PerSeptive Biosystems.

Detection of the intermediate radicals was carried out at the Polymer Department of Moscow State University by ESR spectroscopy using a RE-1307 instrument, equipped with a universal X-band (9.4 GHz) cavity using 100 kHz field modulation, 30 mW microwave power, and amplitude in field modulation 0.03 G. The reaction mixture prepared according to the procedure described above was poured into a molybdenic glass ampule with an inner diameter equal to 1.8 mm. The experiment was carried out at 90 °C directly in the resonator of the spectrometer. Data processing and simulations were carried out using respectively the EPR (v. 2.3) and Bruker EPRSRC software packages. The amount of paramagnetic centers was determined by comparison of the integral of the ESR signal of the sample with that of a carbon black standard of known spin number.

Results

1. Molar Mass Characteristics and Structure of the Polymers. a. Average Molar Mass and Molar Mass Distribution. Whereas classical radical polymerization of *n*-BuA usually leads to the formation of cross-linked insoluble polymer at high conversions (the same was observed for experiments 1g and 3g), in the presence of a sufficient concentration of t-BDB as a RAFT agent, polymerizations proceeded without the formation of gel; i.e., the recovered polymers were always fully soluble (it is for instance the case in experiments 1a−1d and 3a−3c after 60−70% monomer conversion).

Molar mass characteristics were determined for the systems containing 10^{-3} mol L^{-1} of AIBN and different concentrations of t-BDB at 60 °C (experiments 1a−1c) and 90 °C (experiments 3a−3c). Figure 1a shows that for all of the investigated systems, independently of the temperature, M_n increased linearly with monomer conversion, in good agreement with the theory of living/controlled polymerization (theoretical M_n was calculated from the ratio of monomer initial concentration over RAFT agent initial concentration). At the same time the polymers were characterized by low values of the polydispersity indexes (PDI), which remained significantly below 1.5 throughout the polymerization (see Figure 1b). These results fully confirmed that the polymerizations proceeded via a controlled mechanism, which is also illustrated in Figure 2 (experiment 1c) by the shift of the SEC chromatograms toward larger molar masses, with the progress of monomer conversion. However, the quality of control slightly deteriorated at large monomer conversions as shown by the PDI, which extended from 1.07 to 1.20 over a broad conversion range, but increased up to 1.33 at high conversions (Figure 1b). In addition, it can be seen for experiment

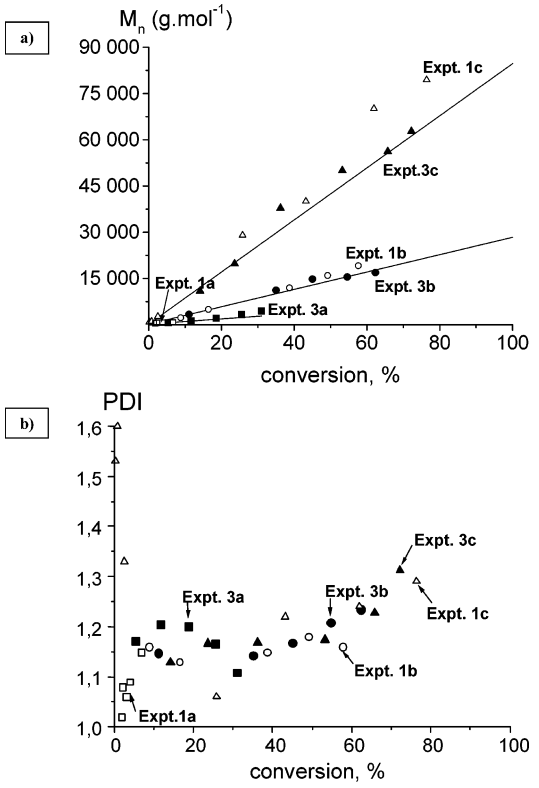

Figure 1. Molar mass (a) and polydispersity index (b) vs conversion for n-BuA polymerizations in bulk with AIBN as an initiator and t-BDB as a reversible chain transfer agent. See Table 1 for experimental conditions. Straight line: $M_n = MW_{t-BDB} + (\text{conv}[M]_0/[\text{t-BDB}]_0)MW_{monomer}$.

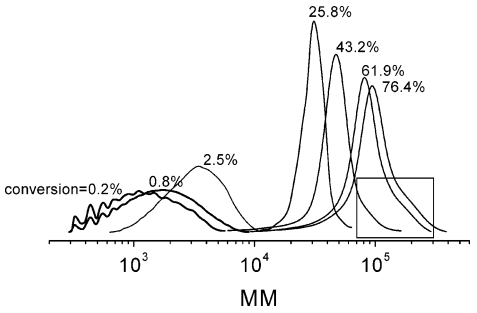

Figure 2. Size exclusion chromatograms of the poly(n-BuA) polymers prepared at 60 °C with AIBN as an initiator and t-BDB as a transfer agent (experiment 1c). $[AIBN]_0 = 10^{-3}$ mol L^{-1}; $[\text{t-BDB}]_0 = 10^{-2}$ mol L^{-1}.

1c after 60% conversion (M_n > 70 000 g mol^{-1}) that M_n simultaneously increased above the theoretical line (Figure 1a) and that a shoulder appeared on the high molar mass side of the chromatograms (Figure 2). The appearance of this shoulder was also observed in experiments 1b, 1e, and 1f, above ∼50−60% conversion. This feature has already been observed in most RAFT polymerizations of alkyl acrylates (see the Introduction) and might be assigned either to branched structures as a result from intermolecular chain transfer to polymer or possibly to cross-termination products.

In RAFT polymerization, the important kinetic parameter that governs the linear increase of molar mass with monomer conversion is C_{tr}, the apparent chain transfer constant to the RAFT agent, namely t-BDB in this work. As shown in Figure 1a, there is a good match between the experimental molar masses and the theoretical ones, even at very low monomer conversions. It is for instance the case for experiments 1a−1c and

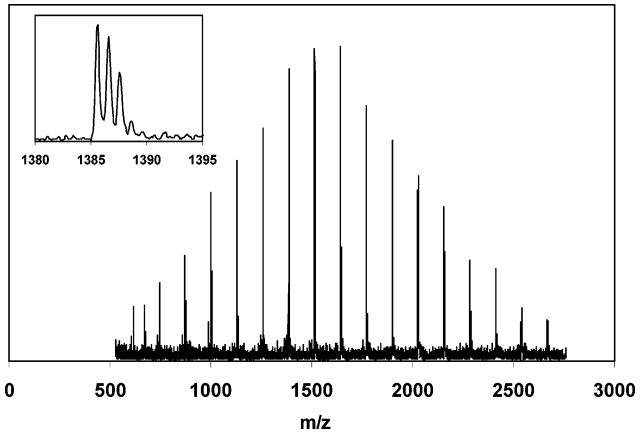

Figure 3. MALDI-TOF-MS spectrum of poly(n-BuA) obtained in experiment 3a at 12% conversion (M_n = 1300 g mol^{-1}; PDI = 1.23).

Scheme 2. Structure of the Poly(*n*-butyl acrylate) Polymer Chains Obtained by Controlled Free-Radical Polymerization in the Presence of t-BDB as a Reversible Chain Transfer Agent

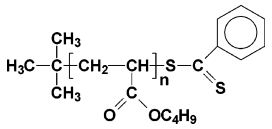

Table 2. Theoretical and Experimental Molar Mass (from MALDI−TOF-MS; Monoisotopic Peak) of Na^+ Ionized Poly(*n*-butyl acrylate) from Experiment 3a (See Scheme 2 for Polymer Structure)

sample characteristics (from SEC)	*n*	theor *m/z*	exptl *m/z*
conv = 12%	9	1385.80	1385.60
M_n = 1300 g mol^{-1}	10	1513.88	1513.59
PDI = 1.23	11	1641.96	1641.70
conv = 19%	12	1770.05	1769.49
M_n = 2200 g mol^{-1}	13	1898.13	1897.61
PDI = 1.20	14	2026.22	2025.66
conv = 26%	15	2154.30	2153.57
M_n = 3300 g mol^{-1}	16	2282.38	2281.70
PDI = 1.17	17	2410.47	2409.73
conv = 31%	18	2538.55	2537.82
M_n = 4500 g mol^{-1}	19	2666.63	2665.97
PDI = 1.11	20	2794.72	2794.10

3a−3c above approximately 3% monomer conversion. This result indicates that the RAFT agent is completely consumed in the early stages of the polymerization and hence that C_{tr} is large. The estimation of C_{tr} using the method suggested by Chong et al.[10] gave us a value of about 100. More accurate determination of C_{tr} by direct measurement of the conversion of both the RAFT agent and the monomer by NMR and gas-phase chromatography is planned.

b. Chain-End Structure Analyzed by MALDI-TOF-MS. Polymers obtained in experiment 3a were examined by MALDI-TOF-MS. A typical spectrum is presented in Figure 3 for a polymer sample exhibiting 12% conversion. A single series could be observed with molar mass between the peaks corresponding to the molar mass of one monomer unit (128.08 u). Comparison of the experimental *m/z* with the calculated molar masses corresponding to the structure in Scheme 2 led to the conclusion that a large majority of the poly(*n*-butyl acrylate) macromolecular chains exhibited the expected structure with the RAFT agent fragments at

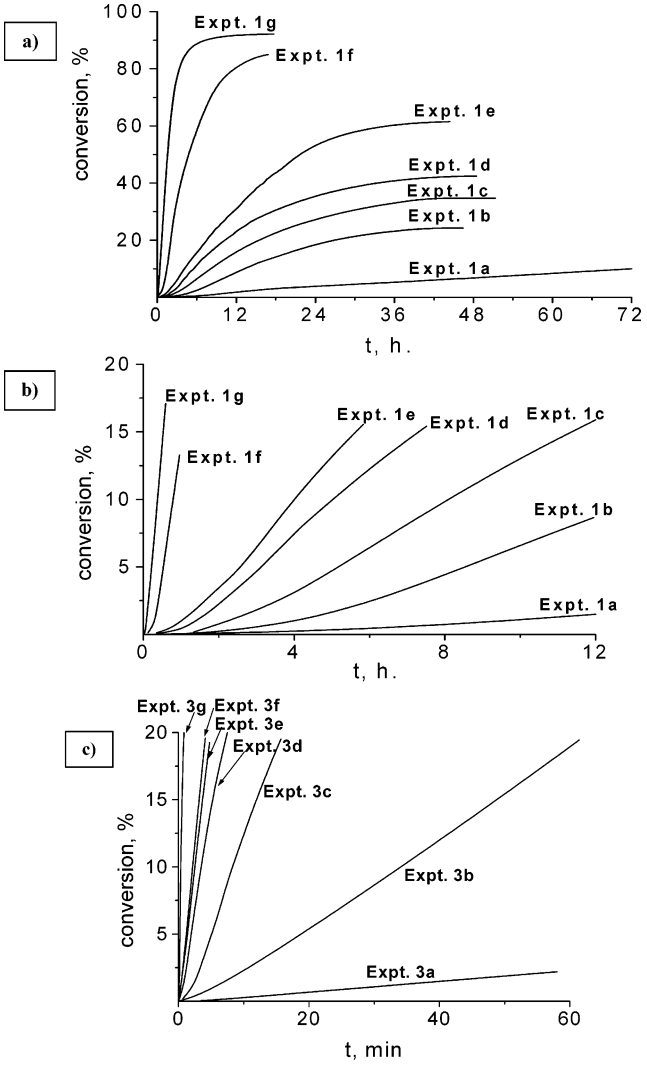

Figure 4. Kinetics of n-BuA polymerization in bulk at 60 °C (a, b) and 90 °C (c) in the presence of AIBN as an initiator and t-BDB as a transfer agent. See Table 1 for experimental conditions.

both ends (see Table 2). In the examined low-conversion samples, no other peak series with cyanoisopropyl end group or with structure corresponding to classical termination product or to 3-arm or 4-arm stars (that would form by termination involving the intermediate radicals) could be detected in the corresponding spectra. This does not mean they did not exist, but simply the experimental conditions were not designed in order to target their observation.

2. Polymerization Kinetics. Figure 4a−c displays the typical kinetic curves of the polymerization of n-BuA in the presence of various concentrations of t-BDB at 60 °C (experiments 1a−1g) and 90 °C (experiments 3a−3g). From Figure 4b at 60 °C it can be seen that all conversion vs time plots exhibited a pronounced S-shape in the presence of CTA, with an induction period that increased with the increase in t-BDB initial concentration (for instance, see experiment 1b; at [t-BDB] = 0.03 mol L^{-1} and 60 °C, polymerization started only after 2 h of heating). Moreover, increasing t-BDB concentration resulted in the significant decrease of the polymerization rate. The same shape was also observed in the polymerizations at 90 °C, but in this case, the induction period was strongly reduced, being usually less than 10 min (Figure 4c, experiments 3a−3f).

From the kinetic analysis, we determined the apparent external orders of the reaction with respect to AIBN and t-BDB concentrations, using for each experiment the maximum value of the polymerization rate, after the induction period. For the experiments conducted at 60 °C and characterized by a long induction period (experiments 1 and 2), the polymerization rate was calculated for the same monomer conversion (the difference in initiator consumption could be neglected due to low value of AIBN decomposition rate constant, i.e., $k_d = 8.5 \times 10^{-6}$ s^{-1}).[44] For experiments 3 and 4 carried out at 90 °C, where the induction period was significantly shorter, calculations have been done for the same polymerization time equal to 10 min. From the dependence of the maximum initial polymerization rate vs the initial concentrations of AIBN and t-BDB (Figure 5, experiments 1−4) the apparent orders with respect to AIBN and t-BDB were determined; they were close to 0.5 and −0.5, respectively, irrespective of the temperature (for t-BDB, they were -0.50 ± 0.10 at 60 °C and -0.59 ± 0.07 at 90 °C, whereas for AIBN, they were 0.52 ± 0.02 at 60 °C and 0.59 ± 0.03 at 90 °C).

3. ESR Analysis of the Reaction Medium at 90 °C. ESR qualitative and quantitative analysis of the intermediate radicals in n-BuA polymerization in the presence of cumyl dithiobenzoate RAFT agent was previously reported by Hawthorne et al.[35] In the present work, the polymerization medium was also analyzed by ESR. Heating the reaction mixture of n-BuA with AIBN and t-BDB at 90 °C resulted, within 15−20 s of heating, in the appearance of a signal, the intensity of which increased with time and was strongly affected by AIBN and t-BDB initial concentrations. The early typical spectrum (Figure 6a) consisted of a 1:3:3:1 quadruplet with complex hyperfine structure. Upon cooling the sample to 60 °C, the signal disappeared completely but reappeared with similar intensity after heating it again up to 90 °C. The signal was the same when n-BuA was replaced by another monomer such as styrene, *N*-vinylpyrrolidone, or vinyl acetate or even when it was replaced by the corresponding deuterated monomers (α*d*-styrene, d_8-styrene, or α*d*-vinyl acetate). These results indicate, as we shall see below, that the α-proton of the polymeric radical added to t-BDB did not significantly influence the hyperfine structure of the resulting adduct radical spectrum. In the absence of added monomer (ESR spectra recorded in benzene or ethylbenzene solutions), the signal intensity was lower by approximately 2 orders of magnitude.

At the early stage of the reaction, it is very likely that the observed spectrum was directly related to the species formed by the addition of an initiating radical or a propagating oligoradical to t-BDB (Scheme 1). In particular, in the presence of monomer, it is reasonable to suppose that the ESR signal mainly corresponded to the addition of an oligomeric radical to t-BDB (Scheme 1B, intermediate radical $I_2^{\bullet}$). The larger concentration of this radical with respect to $I_1^{\bullet}$ formed in the absence of monomer might be justified by either a better chemical stability or a faster rate of formation. The ESR spectrum displayed in Figure 6a after 3 min reaction was thus assigned to the intermediate radical $I_2^{\bullet}$. The general envelope is characteristics of an interaction of the unpaired electron with the hydrogen atoms of the benzene ring. However, this is not sufficient to explain the observed complex hyperfine structure. Since, as it was shown above, the γ-H of the added radical did not affect the ESR spectrum, then it was necessary to assume hyperfine coupling with the δ-H of the leaving *tert*-butyl group. To check this assumption, the spectrum of $I_2^{\bullet}$ was simulated using the following parameters: *g*-factor = 2.0038 G, 9 *tert*-butyl δ-H with $a_{\delta-H} = 0.425$ G, 1 γ-H with $a_{\gamma-H} = 0.1$ G, 2 benzenic ortho-H with $a_{o-H} = 3.65$ G, 2 benzenic meta-H with $a_{m-H} = 1.34$ G, 1 benzenic para-H with $a_{p-H} = 3.99$ G (Figure 6b). A reasonably good fit with the experimental spectrum shown in Figure 6a was observed. The larger hyperfine coupling constant to the δ-H of the *tert*-butyl group with respect to the γ-H of the added oligoradical was rather unexpected and would require further investigation. The absence of strong effect of the γ-H has already been reported by Alberti et al.[46] for the polymerization of styrene in the presence of benzyl (diethoxyphosphoryl)-dithioformate as a RAFT agent.

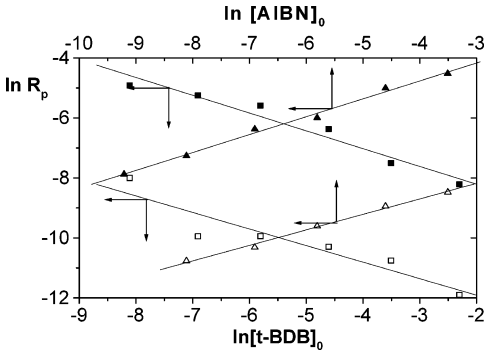

Figure 5. Bilogarithmic plot of polymerization rate (R_p) vs concentration of AIBN or t-BDB at 60 °C (open symbols, experiments 1 and 2) and 90 °C (black symbols, experiments 3 and 4). Effect of $[t\text{-BDB}]_0$: slope = -0.50 ± 0.10 at 60 °C and -0.59 ± 0.07 at 90 °C. Effect of $[AIBN]_0$: slope = 0.52 ± 0.02 at 60 °C and 0.59 ± 0.03 at 90 °C. See Table 1 for experimental conditions.

At longer times, the ESR spectrum gradually deformed (Figure 6c, polymerization time: 20 min; and finally Figure 6d, polymerization time: 100 min) mainly due to the change in radical structure (from $I_2^{\bullet}$ to $I_3^{\bullet}$) and possibly to the increase in chain length and medium viscosity. In particular, the spectrum shown in Figure 6d was assigned to radical $I_3^{\bullet}$ (Scheme 1C). Hyperfine structure was essentially influenced by the interaction between the unpaired electron and the hydrogens of the benzene ring. As mentioned above, negligible splitting resulting from coupling to the two γ-H from the attached polymer chains was detected. This was corroborated by simulation (Figure 6e, *g*-factor = 2.0043 G, 2 γ-H with $a_{\gamma-H} = 0.1$ G, 2 benzenic ortho-H with $a_{o-H} = 3.66$ G, 2 benzenic meta-H with $a_{m-H} = 1.34$ G, 1 benzenic para-H with $a_{p-H} = 3.96$ G). Assignment of the spectrum shown in Figure 6d was further confirmed by the results obtained with poly(n-BuA) taken as a RAFT agent. When poly(n-BuA) was isolated after polymerization, purified, and then used as a RAFT agent in the polymerization of a new portion of freshly distilled monomer, the ESR spectrum observed at 90 °C and supposed to correspond to radical $I_3^{\bullet}$ was exactly the same as that displayed in Figure 6d. The same spectrum was also previously observed in the polymerization of n-BuA in the presence of cumyl dithiobenzoate as a RAFT agent.[35] Since this RAFT agent differs from t-BDB by only the nature of the leaving group, structures of the intermediate radicals $I_3^{\bullet}$ should be identical in both cases, which explains the similarity in the ESR spectra.

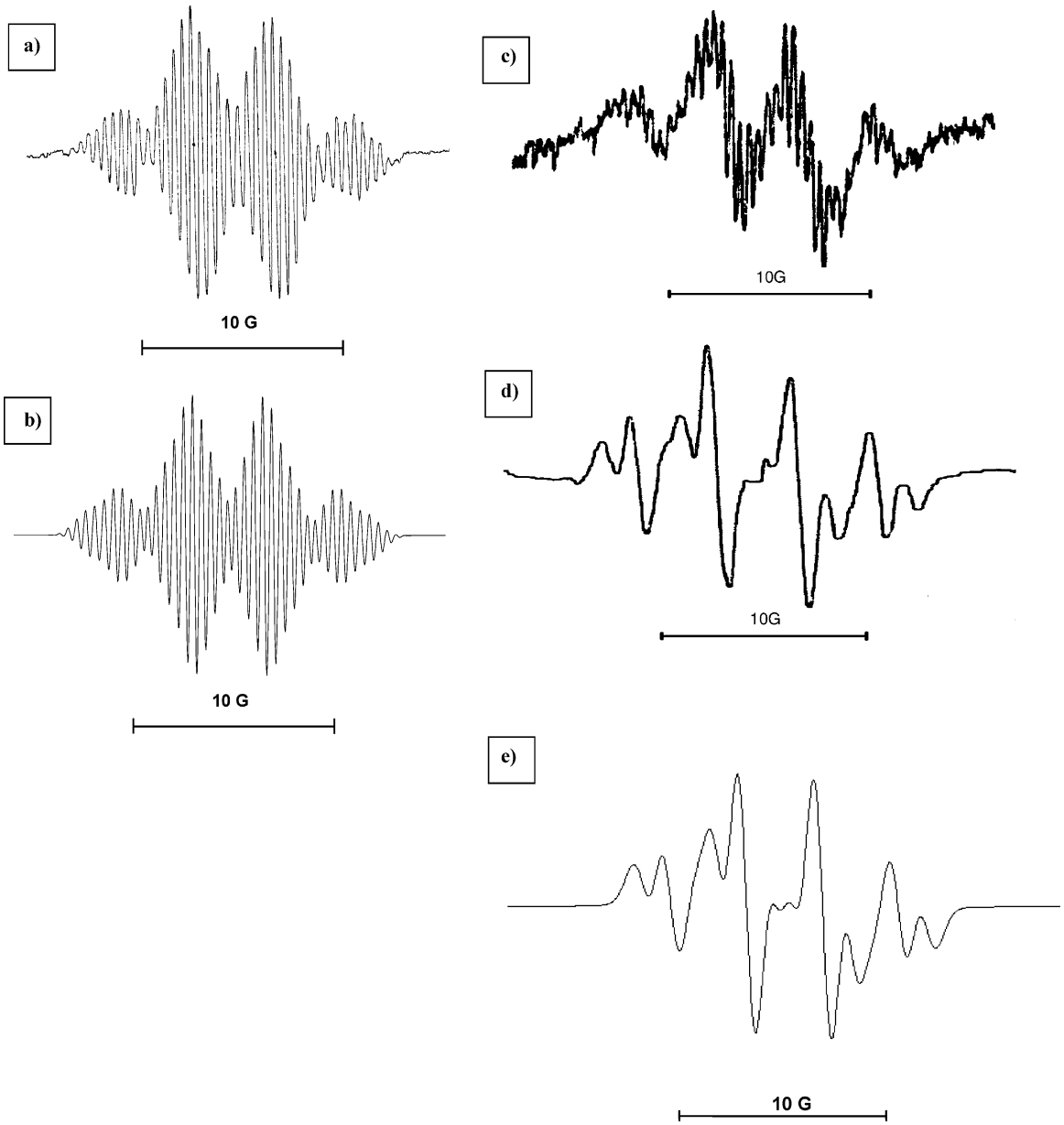

Figure 6. ESR spectra of the intermediate radicals formed in experiment 5a at 90 °C. (a) Experimental; time = 3 min. (b) Simulation (g = 2.0038 G, 9 *tert*-butyl δ-H with $a_{\delta-H}$ = 0.425 G, 1 γ-H with $a_{\gamma-H}$ = 0.1 G, 2 benzenic ortho-H with a_{o-H} = 3.65 G, 2 benzenic meta-H with a_{m-H} = 1.34 G, 1 benzenic para-H with a_{pH} = 3.99 G). The line width of the spectrum was set to 0.18 G, and the line shape was Lorentzian/Gaussian = 0.5. (c) Experimental; time = 20 min. (d) Experimental; time = 100 min. (e) Simulation (g = 2.0043 G, 2 γ-H with $a_{\gamma-H}$ = 0.1 G, 2 benzenic ortho-H with a_{o-H} = 3.66 G, 2 benzenic meta-H with a_{m-H} = 1.34 G, 1 benzenic para-H with a_{p-H} = 3.96 G). The line width of the spectrum was set to 1.08 G, and the line shape was Lorentzian/Gaussian = 0.8.

The influence of the concentrations of AIBN and t-BDB on the kinetics of formation of the intermediate radicals $I_2^\bullet$ and $I_3^\bullet$ at 90 °C is displayed in Figure 7a,b (the overall concentration was given owing to superimposed ESR signals). All of the kinetic curves can be divided into two parts, as already observed previously for styrene.[47,48] At the beginning the overall concentration of intermediate radicals increased with time, reached a maximum concentration, and then decreased. The time to reach the maximum increased when $[t\text{-BDB}]_0$ was increased or when $[AIBN]_0$ was decreased. The maximum concentration of intermediate radicals increased with the increase in both AIBN and t-BDB initial concentrations; it was in the 0.2×10^{-5}–1.5×10^{-5} mol L^{-1} range for the studied experiments (experiments 5a–5d, 6, and 7). Such a concentration is unexpectedly large for a free radical species; it is larger by 1–2 orders of magnitude than the concentration reported for n-BuA polymerization in the presence of cumyl dithiobenzoate.[35]

Discussion

The presented experimental results concerning the polymerization kinetics might give useful information on the mechanism of the n-BuA/t-BDB polymerization system proceeding via RAFT. They are discussed in this part, in particular, (i) the existence of an induction period, (ii) the large concentration of intermediate radicals in the early stage of the reaction, and (iii) the rate retardation accompanied by a −0.5th order of the polymerization rate with respect to the RAFT agent. On the basis of the previous literature, all those results have to be examined considering either the possibility of cross-termination with fast fragmentation or the

absence of cross-termination, but slow fragmentation. All kinetic equations with definition of the terms used are reported in the Appendix at the end of this article.

Induction Period. The ESR experiments showed that in the earliest part of the polymerization the intermediate radicals, I•, accumulated in the reaction medium, i.e., $d[I^\bullet]/dt > 0$. On the basis of the kinetic analysis (see Appendix), the evolution with time of the concentration of the propagating radicals P• reads as shown in eq 1 (from eq A11 in the Appendix or Eq A22 when $k'_t = 0$), where R_i is the initiation rate, k_t the rate constant of termination between propagating macroradicals, and k'_t the rate constant of cross-termination between a propagating macroradical and a I• adduct radical.

$$\frac{d[P^\bullet]}{dt} = R_i - k_t[P^\bullet]^2 - 2k'_t[P^\bullet][I^\bullet] - \frac{d[I^\bullet]}{dt} \qquad (1)$$

Consequently, during the I• accumulation period, the concentration of the propagating radical P• would increase quite slowly and remain lower than in a similar reaction carried out in the absence of RAFT agent. Such situation should persist as long as $d[I^\bullet]/dt > 0$. Therefore, the initial formation of the intermediate radicals might be the cause of the existence of an induction period and of the observed S-shaped conversion vs time plots, without the need to invoke cross-termination to explain it. Such behavior is compatible with slow fragmentation, but the experimental results do not allow, at that stage, to give an estimation of the extent of the fragmentation rate constant. The rate of addition of the propagating radicals to the thiocarbonyl groups of the RAFT agents, i.e., $k_{add}[P^\bullet][RX]$ and $k'_{add}[P^\bullet][PX]$, also played an important contribution in the kinetics of that period (see Scheme 1; RX = t-BDB, PX = polymer chain terminated by the dithiobenzoate end group).

In contrast, the selectivity proposed by McLeary et al.,[34] which would initially form a larger proportion of the initiating *tert*-butyl radical with respect to P•, might not lead in our case to an initialization period with reduced propagation rate. Indeed, the rate constant of addition of the *tert*-butyl radical to an acrylate monomer (k_{p1}) is larger than the rate constant of propagation of *n*-butyl acrylate, k_p ($k_{p1} = 1.7 \times 10^6$ L mol^{-1} s^{-1} for the addition of the *tert*-butyl radical to methyl acrylate at 60 °C,[49] whereas $k_p = 3.4 \times 10^4$ L mol^{-1} s^{-1} for the propagation of *n*-butyl acrylate at 60 °C[50]). Consequently, the expelled *tert*-butyl radical might add at least one monomer unit, and the formed oligoradical would then react quite rapidly with the t-BDB chain transfer agent to produce the intermediate radical $I_2^\bullet$.

Maximum Concentration of the Intermediate Radicals. The large concentration of I• measured at the maximum increased with the increase in both AIBN and t-BDB initial concentrations. This is in good qualitative agreement with the theoretical predictions (see Appendix). This large concentration of intermediate radicals might initially correspond to a large concentration of $I_2^\bullet$, caused by large AIBN and t-BDB initial concentrations (see Figure 7 and Table 1) together with a large preequilibrium constant $k_{add}/(k_{-add} + k_{fr})$. In the studied n-BuA/t-BDB system, k_{add}, the addition rate constant of an acrylate terminated oligomer to t-BDB, might be quite large (possibly larger than k_p by 1 or 2 orders of magnitude, if one considers the fast consumption of t-BDB discussed at the beginning of this article).

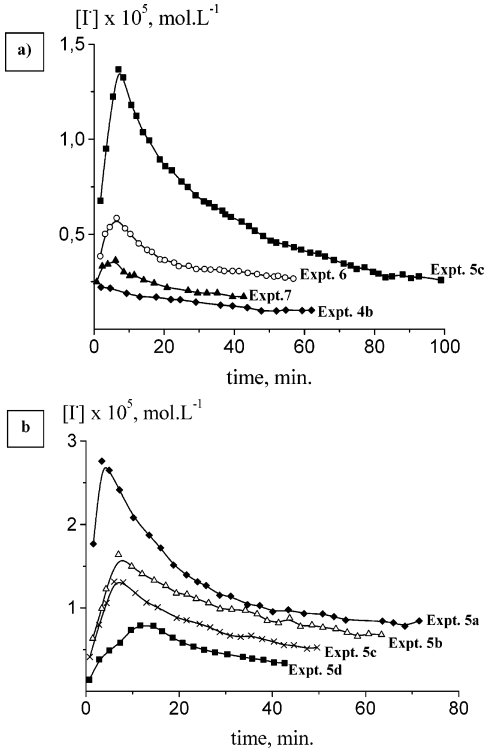

Figure 7. Overall concentration of the intermediate radicals vs time in n-BuA polymerization with AIBN as an initiator and t-BDB as a transfer agent at 90 °C: (a) $[AIBN]_0 = 10^{-2}$ mol L^{-1}, effect of $[t\text{-BDB}]_0$. (b) $[t\text{-BDB}]_0 = 3 \times 10^{-1}$ mol L^{-1}, effect of $[AIBN]_0$. See Table 1 for experimental conditions.

Simultaneously, the $(k_{-add} + k_{fr})$ value might be smaller than for the polymerization of styrene, indicating a slower fragmentation. It is however not possible from our experimental data to conclude on the absolute range of the fragmentation rate constants.

Polymerization Rate. It was shown by Kwak et al.[27,32] that cross-termination can explain the rate retardation observed in the polymerizations based on RAFT, in agreement with the following equation describing the stationary concentration of propagating radicals as a function of initiator and RAFT agent initial concentrations (see Appendix for the complete kinetic analysis; eqs A1−A16).

$$[P^\bullet] = \left(\frac{R_i/k_t}{1 + 2\,\frac{k'_t}{k_t} K_{app}[RX]_0} \right)^{1/2} \qquad (2)$$

The kinetic data determined after the induction period (i.e., 0.5th and −0.5th order with respect to AIBN and t-BDB, respectively) are in good agreement with such calculated stationary concentration of propagating radicals.

In the absence of cross-termination, the concentration of propagating radicals would be lower than in a classical system as long as the intermediate radicals accumulate (i.e., $d[I^\bullet]/dt > 0$). However, after the maximum concentration in I•, no rate retardation is expected. Indeed, on the basis of eq 1 and of the equations given in the Appendix, when $d[I^\bullet]/dt < 0$, [P•] should not be reduced with respect to a similar polymerization in the absence of RAFT agent, considered at the same polymerization time (same R_i).

Conclusions

The RAFT polymerization of *n*-butyl acrylate was studied in the presence of various concentrations of *tert*-butyl dithiobenzoate (t-BDB) as a chain transfer agent and various concentrations of AIBN initiator at 60 and 90 °C. The polymerizations exhibited the expected features of a controlled system. In particular, the linear increase in number-average molar mass (M_n) with monomer conversion, from very low conversion values, indicated a large chain transfer constant to t-BDB. The kinetic study showed two typical characteristics already observed in RAFT polymerizations of acrylates: the existence of an induction period and a strong rate retardation, both enhanced by the increase in t-BDB initial concentration. ESR spectroscopy was applied at 90 °C and revealed the existence of an unexpectedly large concentration of intermediate radicals. In the early stage of the polymerization, such a radical was attributed to that formed in the preequilibrium by the direct addition of poly(*n*-butyl acrylate) oligoradical to t-BDB ($I_2^\bullet$). With the progress of monomer conversion and t-BDD consumption, it changed into $I_3^\bullet$, containing two polymeric fragments attached to the sulfur atoms.

All the kinetics features of the n-BuA/t-BDB system were examined considering two potential interpretations: either the possibility of cross-termination with fast fragmentation or the absence of cross-termination, but slow fragmentation. It appeared that the induction period was not caused by a selectivity in radical addition, but by an initially slow increase in the concentration of the propagating radicals, due to the concomitant formation of the intermediate radicals. Such behavior was rather compatible with a slow fragmentation, at least of the intermediate radical $I_2^\bullet$. In the same way, the high concentration of intermediate radicals was explained by a high apparent equilibrium constant, which is also compatible with slow fragmentation, together with fast addition of the propagating radicals to the t-BDB RAFT agent. The further rate retardation was however better explained by the existence of cross-termination.

Acknowledgment. The authors are indebted to the French Ministery of Research and Technology for the financial support of E. Chernikova. This research was also supported by the Russian Foundation for Basic Research (Project 02-03-32183). They thank J. Belleney from UPMC for the MALDI-TOF mass spectrometry analyses. B.C. is personally grateful to Dr. L. Marx and Prof. A. Rassat for interesting and fruitful discussions.

Appendix

1. First Case: Existence of Cross-Termination along with Fast Fragmentation of the Intermediate Radicals. The Steady-State Conditions Apply for Both the Propagating and the Intermediate Radicals. Consider that the addition−fragmentation equilibrium starts from the second step (Scheme 1B), with RX the RAFT agent, PX the polymer chains terminated by the dithiobenzoate end group, $P^\bullet$ = t-Bu-(n-BuA)$_i^\bullet$, or $P^\bullet$ = NC-C(CH$_3$)$_2$-(n-BuA)$_i^\bullet$ (with i = 1, 2, 3, ... small value) the propagating radical, and $I_2^\bullet$ and $I_3^\bullet$ the intermediate radicals ($[I^\bullet] = [I_2^\bullet] + [I_3^\bullet]$).

$$\frac{d[I_2^\bullet]}{dt} = k_{add}[P^\bullet][RX] - (k_{-add} + k_{fr})[I_2^\bullet] - k'_t[P^\bullet][I_2^\bullet] \quad (A1)$$

$$\frac{d[I_3^\bullet]}{dt} = k'_{add}[P^\bullet][PX] - 2k'_{-add}[I_3^\bullet] - k'_t[P^\bullet][I_3^\bullet] \quad (A2)$$

$$\frac{d[I^\bullet]}{dt} = \frac{d[I_2^\bullet]}{dt} + \frac{d[I_3^\bullet]}{dt} = k_{add}[P^\bullet][RX] - (k_{-add} + k_{fr})[I_2^\bullet] - k'_t[P^\bullet][I_2^\bullet] + k'_{add}[P^\bullet][PX] - 2k'_{-add}[I_3^\bullet] - k'_t[P^\bullet][I_3^\bullet] \quad (A3)$$

$$\frac{d[I^\bullet]}{dt} = (k_{add}[RX] + k'_{add}[PX])[P^\bullet] - (k_{-add} + k_{fr})[I_2^\bullet] - 2k'_{-add}[I_3^\bullet] - k'_t[P^\bullet]([I_2^\bullet] + [I_3^\bullet]) \quad (A4)$$

$$\frac{d[I^\bullet]}{dt} = \left(k_{add}\frac{[RX]}{[RX]_0} + k'_{add}\frac{[PX]}{[RX]_0}\right)[RX]_0[P^\bullet] - \left((k_{-add} + k_{fr})\frac{[I_2^\bullet]}{[I^\bullet]} + 2k'_{-add}\frac{[I_3^\bullet]}{[I^\bullet]}\right)[I^\bullet] - k'_t[P^\bullet][I^\bullet] \quad (A5)$$

$$\frac{d[I^\bullet]}{dt} = k_{add,app}[P^\bullet][RX]_0 - k_{fr,app}[I^\bullet] - k'_t[P^\bullet][I^\bullet] \quad (A6)$$

R_i is the initiation rate, k_t the rate constant of termination between propagating macroradicals, and k'_t the rate constant of cross-termination between a propagating macroradical and a $I^\bullet$ adduct radical. $[RX]_0$ is the initial concentration of the RAFT agent (i.e., t-BDB in this work; R = *tert*-butyl and X = dithiobenzoate). The apparent rate constants of addition and fragmentation are respectively

$$k_{add,app} = k_{add}\frac{[RX]}{[RX]_0} + k'_{add}\frac{[PX]}{[RX]_0} \quad (A7)$$

$$k_{fr,app} = (k_{-add} + k_{fr})\frac{[I_2^\bullet]}{[I^\bullet]} + 2k'_{-add}\frac{[I_3^\bullet]}{[I^\bullet]} \quad (A8)$$

The evolution rate of the propagating macroradical concentration with time can then be expressed as follows:

$$\frac{d[P^\bullet]}{dt} = R_i - k_t[P^\bullet]^2 - k'_t[P^\bullet][I^\bullet] - k_{add}[P^\bullet][RX] + (k_{-add} + k_{fr})[I_2^\bullet] - k'_{add}[P^\bullet][PX] + 2k'_{-add}[I_3^\bullet] \quad (A9)$$

$$\frac{d[P^\bullet]}{dt} = R_i - k_t[P^\bullet]^2 - 2k'_t[P^\bullet][I^\bullet] - \frac{d[I_2^\bullet]}{dt} - \frac{d[I_3^\bullet]}{dt} \quad (A10)$$

$$\frac{d[P^\bullet]}{dt} = R_i - k_t[P^\bullet]^2 - 2k'_t[P^\bullet][I^\bullet] - \frac{d[I^\bullet]}{dt} \quad (A11)$$

In all those equations the homotermination between two intermediate radicals was not considered.[32] In addition, fast reinitiation by the expelled *tert*-butyl radical was supposed, owing to a very large rate constant of addition to the monomer[49] and to a large initial concentration of the latter.

When the overall concentration of intermediate radicals reaches the steady state (at and after the maximum concentration), the following equations can be written:

$$\frac{d[I^\bullet]}{dt} = k_{add,app}[P^\bullet][RX]_0 - k_{fr,app}[I^\bullet] - k'_t[P^\bullet][I^\bullet] = 0 \quad (A12)$$

$$[I^\bullet] = \frac{k_{add,app}}{k_{fr,app} + k'_t[P^\bullet]}[P^\bullet][RX]_0 \quad (A13)$$

Only if fragmentation is fast enough with respect to cross-termination can the following simplified equation be written, with K_{app} the apparent equilibrium constant.

$$[I^\bullet] = \frac{k_{add,app}[P^\bullet][RX]_0}{k_{fr,app}} = K_{app}[P^\bullet][RX]_0 \quad (A14)$$

Then, according to the equations below, the concentration of the propagating radicals should undergo reduction with respect to a classical polymerization conducted in the absence of RX, only if cross-termination occurs.[27,32]

$$\frac{d[P^\bullet]}{dt} = R_i - k_t[P^\bullet]^2 - 2k'_t[P^\bullet][I^\bullet] = 0 \quad (A15)$$

$$[P^\bullet] = \left(\frac{R_i/k_t}{1 + 2\frac{k'_t}{k_t}K_{app}[RX]_0}\right)^{1/2} = r(R_i/k_t)^{1/2} \quad (A16)$$

The term r corresponds to a retardation factor, which can be defined as $r = (1 + 2(k'_t/k_t)K_{app}[RX]_0)^{-1/2}$, where R_i is the initiation rate proportional to $[AIBN]_0$.

Similarly, the concentration of intermediate radicals can be written in the following way.

$$[I^\bullet] = K_{app}[P^\bullet][RX]_0 = K_{app}[RX]_0\left(\frac{R_i/k_t}{1 + 2\frac{k'_t}{k_t}K_{app}[RX]_0}\right)^{1/2} \quad (A17)$$

The decrease in $[I^\bullet]$ with time, after the maximum, might then be assigned to a decrease in R_i, owing to the fast consumption of AIBN at 90 °C.

2. Second Case: Cross-Termination Does Not Exist; Steady-State Conditions Do Not Apply for the Intermediate Radicals. If cross-termination does not exist, the only way to explain rate retardation is to consider a slow fragmentation process; in that case, steady-state concentrations of the intermediate radicals cannot be considered anymore.

$$\frac{d[I_2^\bullet]}{dt} = k_{add}[P^\bullet][RX] - (k_{-add} + k_{fr})[I_2^\bullet] \quad (A18)$$

$$\frac{d[I_3^\bullet]}{dt} = k'_{add}[P^\bullet][PX] - 2k'_{-add}[I_3^\bullet] \quad (A19)$$

$$\frac{d[I^\bullet]}{dt} = \frac{d[I_2^\bullet]}{dt} + \frac{d[I_3^\bullet]}{dt} = k_{add,app}[P^\bullet][RX]_0 - k_{fr,app}[I^\bullet] \quad (A20)$$

$$\frac{d[P^\bullet]}{dt} = R_i - k_t[P^\bullet]^2 - k_{add}[P^\bullet][RX] + (k_{-add} + k_{fr})[I_2^\bullet] - k'_{add}[P^\bullet][PX] + 2k'_{-add}[I_3^\bullet] \quad (A21)$$

$$\frac{d[P^\bullet]}{dt} = R_i - k_t[P^\bullet]^2 - \frac{d[I^\bullet]}{dt} \quad (A22)$$

At the maximum concentration of $[I^\bullet]$

$$\frac{d[I^\bullet]}{dt} = 0 \quad (A23)$$

$$k_{add,app}[P^\bullet][RX]_0 - k_{fr,app}[I^\bullet] = 0 \quad (A24)$$

$$[I^\bullet]_{max} = \frac{k_{add,app}[P^\bullet][RX]_0}{k_{fr,app}} = K_{app}[P^\bullet][RX]_0 \quad (A25)$$

At this stage, if one considers steady-state conditions for the propagating radicals

$$\frac{d[P^\bullet]}{dt} = R_i - k_t[P^\bullet]^2 - \frac{d[I^\bullet]}{dt} = R_i - k_t[P^\bullet]^2 = 0 \quad (A26)$$

and then

$$[P^\bullet] = (R_i/k_t)^{1/2} \quad (A27)$$

This leads to

$$[I^\bullet]_{max} = K^{app}\left(\frac{R_i}{k_t}\right)^{1/2}[RX]_0 \quad (A28)$$

Before the maximum in intermediate radicals concentration, $d[I^\bullet]/dt > 0$, whereas after the maximum, $d[I^\bullet]/dt < 0$. In this latter stage, the production of propagating radical would be faster at a given polymerization time than in the same polymerization conducted without any RAFT agent. A larger than expected concentration might then be observed ($[P^\bullet] > (R_i/k_t)^{1/2}$).

References and Notes

(1) *Controlled Radical Polymerization*; Matyjaszewski, K., Ed.; *ACS Symp. Ser.* **1998**, *685*.
(2) *Controlled/Living Radical Polymerization: Progress in ATRP, NMP, and RAFT*; Matyjaszewski, K., Ed.; *ACS Symp. Ser.* **2000**, *768*.
(3) *Advances in Controlled/Living Radical Polymerization*; Matyjaszewski, K., Ed.; *ACS Symp. Ser.* **2003**, *854*.
(4) Hawker, C. J.; Bosman, A. W.; Harth, E. *Chem. Rev.* **2001**, *101*, 3661.
(5) Matyjaszewski, K.; Xia, J. *Chem. Rev.* **2001**, *101*, 2921.
(6) Kamigaito, M.; Ando, T.; Sawamoto, M. *Chem. Rev.* **2001**, *101*, 3689.
(7) Chiefari, J.; Chong, Y. K. B.; Ercole, F.; Krstina, J.; Jeffery, J.; Le, T. P. T.; Mayadunne, R. T. A.; Meijs, G. F.; Moad, C. L.; Moad, G.; Rizzardo, E.; Thang, S. H. *Macromolecules* **1998**, *31*, 5559.
(8) Mayadunne, R. T. A.; Rizzardo, E.; Chiefari, J.; Chong, Y. K.; Moad, G.; Thang, S. H. *Macromolecules* **1999**, *32*, 6977.
(9) Moad, G.; Chiefari, J.; Chong, Y. K.; Krstina, J.; Mayadunne, R. T. A.; Postma, A.; Rizzardo, E.; Thang, S. H. *Polym. Int.* **2000**, *49*, 993.
(10) Chong, Y. K.; Krstina, J.; Le, T. P. T.; Moad, G.; Postma, A.; Rizzardo, E.; Thang, S. H. *Macromolecules* **2003**, *36*, 2256.
(11) Chiefari, J.; Mayadunne, R. T. A.; Moad, C. L.; Moad, G.; Rizzardo, E.; Postma, A.; Skidmore, M. A.; Thang, S. H. *Macromolecules* **2003**, *36*, 2273.
(12) Charmot, D.; Corpart, P.; Adam, H.; Zard, S. Z.; Biadatti, T.; Bouhadir, G. *Macromol. Symp.* **2000**, *150*, 23.

(13) Rizzardo, E.; Chiefari, J.; Mayadunne, R. T. A.; Moad, G.; Thang, S. H. *ACS Symp. Ser.* **2000**, *768*, 278.
(14) Moad, G.; Mayadunne, R. T. A.; Rizzardo, E.; Skidmore, M.; Thang, S. H. *ACS Symp. Ser.* **2003**, *854*, 520.
(15) Chiefari, J.; Rizzardo, E. In *Handbook of Radical Polymerization;* Matyjaszewski, K., Davis, T. P., Eds.; John Wiley and Sons: New York, 2002; p 629.
(16) Lowe, A. B.; McCormick, C. L. *Aust. J. Chem.* **2002**, *55*, 367.
(17) Favier, A.; Charreyre, M. T.; Chaumont, P.; Pichot, C. *Macromolecules* **2002**, *35*, 8271.
(18) D'Agosto, F.; Hughes, R.; Charreyre, M. T.; Pichot, C.; Gilbert, R. G. *Macromolecules* **2003**, *36*, 621.
(19) Ladavière, C.; Dörr, N.; Claverie, J. P. *Macromolecules* **2001**, *34*, 5370.
(20) Loiseau, J.; Dörr, N.; Suau, J. M.; Egraz, J. B.; Llauro, M. F.; Ladavière, C.; Claverie, J. *Macromolecules* **2003**, *36*, 3066.
(21) Barner-Kowollik, C.; Quinn, J. F.; Morsley, D. R.; Davis, T. P. *J. Polym. Sci., Part A: Polym. Chem.* **2001**, *39*, 1353.
(22) Barner-Kowollik, C.; Quinn, J. F.; Nguyen, T. L. U.; Heuts, J. P. A.; Davis, T. P. *Macromolecules* **2001**, *34*, 7849.
(23) Vana, P.; Davis, T. P.; Barner-Kowollik, C. *Macromol. Theory Simul.* **2002**, *11*, 823.
(24) Coote, M. L.; Radom, L. *J. Am. Chem. Soc.* **2003**, *125*, 1490.
(25) Barner-Kowollik, C.; Coote, M. L.; Davis, T. P.; Radom, L. Vana, P. *J. Polym. Sci., Part A: Polym. Chem.* **2003**, *41*, 2828.
(26) Wang, A. R.; Zhu, S.; Kwak, Y.; Goto, A.; Fukuda, T.; Monteiro, M. S. *J. Polym. Sci., Part A: Polym. Chem.* **2003**, *41*, 2833.
(27) Kwak, Y.; Goto, A.; Tsujii, Y.; Murata, Y.; Komatsu, K.; Fukuda, T. *Macromolecules* **2002**, *35*, 3026.
(28) Ah Toy, A.; Vana, P.; Davis, T. P.; Barner-Kowollik, C. *Macromolecules* **2004**, *37*, 744.
(29) De Brouwer, H.; Schellekens, M. A. J.; Klumperman, B.; Monteiro, M. J.; German, A. L. *J. Polym. Sci., Part A: Polym. Chem.* **2000**, *38*, 3596.
(30) Monteiro, M. J.; de Brouwer, H. *Macromolecules* **2001**, *34*, 349.
(31) Calitz, F. M.; McLeary, J. B.; McKenzie, J. M.; Tonge, M. P.; Klumperman, B.; Sanderson, R. D. *Macromolecules* **2003**, *36*, 9687.
(32) Kwak, Y.; Goto, A.; Fukuda, T. *Macromolecules* **2004**, *37*, 1219.
(33) Kwak, Y.; Goto, A.; Komatsu, K.; Fukuda, T. *Macromolecules* **2004**, *37*, in press.
(34) McLeary, J. B.; Calitz, F. M.; McKenzie, J. M.; Tonge, M. P.; Sanderson, R. D.; Klumperman, B. *Macromolecules* **2004**, *37*, 2483.
(35) Hawthorne, D. G.; Moad, G.; Rizzardo, E.; Thang, S. H. *Macromolecules* **1999**, *32*, 5457.
(36) Bai, R.-K.; You, Y.-Z.; Pan, C.-Y. *Polym. Int.* **2000**, *49*, 898.
(37) Quinn, J. F.; Rizzardo, E.; Davis, T. P. *Chem. Commun.* **2001**, *11*, 1044.
(38) Perrier, S.; Barner-Kowollik, C.; Quinn, J. F.; Vana, P.; Davis, T. P. *Macromolecules* **2002**, *35*, 8300.
(39) Nasrullah, M. J.; Raghunadh, V.; Benicewicz, B. C. *Am. Chem. Soc. Polym. Prepr.* **2003**, *44*, 764.
(40) Kanagasabapathy, S.; Sudalai, A.; Benicewicz, B. C. *Macromol. Rapid Commun.* **2001**, *22*, 1076.
(41) Butté, A.; Storti, G.; Morbidelli, M. *Macromolecules* **2001**, *34*, 5885.
(42) Severac, R.; Lacroix-Desmazes, P.; Boutevin, B. *Polym. Int.* **2002**, *51*, 1117.
(43) Favier, A.; Charreyre, M. T.; Chaumont, P.; Pichot, C. *Macromolecules* **2002**, *35*, 8271.
(44) *Polymer Handbook*, 4th ed.; Brandrup, J., Immergut, E. H., Grulke, E. A., Eds.; John Wiley and Sons: New York, 1999.
(45) The polystyrene calibration is appropriate for poly(*n*-butyl acrylate) samples as shown by the Mark−Houwink−Sakurada parameters: actually, it leads to an error of about 3−5%, which is within the accepted range for SEC analysis. Indeed, the MHS parameters in THF at 30 °C are the following: $K_{PS} = 11.4 \times 10^{-5}$ dL g^{-1} and $\alpha_{PS} = 0.716$ for polystyrene [see: Hutchinson, R. A.; Paquet, D. A., Jr.; McMinn, J. H.; Beuermann, S.; Fuller, R. E.; Jackson, C. *Dechema Monogr.* **1995**, *131*, 467]; $K_{PnBuA} = 12.2 \times 10^{-5}$ dL g^{-1} and $\alpha_{PnBuA} = 0.700$ for poly(*n*-butyl acrylate) [see: Beuermann, S.; Paquet, D. A., Jr.; McMinn, J. H.; Hutchinson, R. A. *Macromolecules* **1997**, *29*, 1918].
(46) Alberti, A.; Benaglia, M.; Laus, M.; Macciantelli, D.; Sparnacci, K. *Macromolecules* **2003**, *36*, 736.
(47) Calitz, F. M.; Tonge, M. P.; Sanderson, R. D. *Macromolecules* **2003**, *36*, 5.
(48) Calitz, F. M.; Tonge, M. P.; Sanderson, R. D. *Macromol. Symp.* **2003**, *193*, 277.
(49) Fischer, H.; Radom, L. *Angew. Chem., Int. Ed.* **2001**, *40*, 1340.
(50) Beuermann, S.; Buback, M. *Prog. Polym. Sci.* **2002**, *27*, 191.

MA049757R